Microfluid Nanofluid (2014) 16:29–37
DOI 10.1007/s10404-013-1198-5

RESEARCH PAPER

Disk-like hydrogel bead-based immunofluorescence staining toward identification and observation of circulating tumor cells

Bo Cai · Feng Guo · Libo Zhao · Rongxiang He · Boran Chen · Zhaobo He · Xiaolei Yu · Shishang Guo · Bin Xiong · Wei Liu · Xingzhong Zhao

Received: 27 December 2012 / Accepted: 29 April 2013 / Published online: 19 May 2013

Abstract Assays toward analysis of rare heterogeneous cells among identical specimen raise a significant challenge in many cell biological studies and clinical diagnosis applications. In this work, we report a disk-like hydrogel bead-based stratagem for rare cell researches at single cell level after a facile microfluidic-based particle synthesis approach. Cells of interested can be encapsulated into alginate droplets which are subsequently solidified into disk-like calcium alginate hydrogel beads and the bead size and cell number inside can be precisely controlled. Due to stability, permeability and disk-like shape of calcium alginate beads, cells immobilized in the disk-like beads can be treated with different chemicals with limited mechanical or fluidic operation influences and observed without distortion comparing with conventional methods or droplet microfluidic methods. Identification of circulating tumor cells, related to early-stage cancer diagnosis, is targeted to demonstrate the potential of our technique in rare cell analysis. This hydrogel bead-based stratagem is performed in immunofluorescence staining treatment and observation of cancer cells from normal hematological cells in blood sample. This method would have a great potential in single cell immobilization, manipulations and observation for biochemical cellular assays of rare cells.

Keywords Microfluidics · Disk-like hydrogel beads · Cell encapsulation · Immunofluorescence staining

B. Cai · R. He · Z. He · X. Yu · S. Guo · W. Liu (✉) · X. Zhao
Key Laboratory of Artificial Micro- and Nano-structures of Ministry of Education, School of Physics and Technology, Wuhan University, Wuhan, People's Republic of China
e-mail: wliu@whu.edu.cn

F. Guo
Department of Engineering Science and Mechanics, Pennsylvania State University, University Park, PA 16802, USA

L. Zhao
Key Laboratory of Molecular Nanostructures and Nanotechnology, Institute of Chemistry, Chinese Academy of Sciences, Beijing, People's Republic of China

B. Chen · B. Xiong
The 2nd School of Clinical Medicine, Wuhan University, Wuhan, People's Republic of China

1 Introduction

Cellular heterogeneity of a tiny minority cells within a genetically identical population reveals potential origins, development and progression of many diseases (Asano et al. 1996; Sugars and Rubinsztein 2003; Zhu et al. 2012; Zhang et al. 2012a). Among more and more important investigations of these precious rare cells in fundamental biological researches, pathology and clinical diagnostics, studies of circulating tumor cells (CTCs) in oncology are representative (Gupta and Massagué 2006). Although CTCs are very few in peripheral blood stream relative to the amount of hematological cells (a few to hundreds in 10^9/mL hematological cells), they are thought to be the key to understand metastasis mechanisms of cancers and detect cancers in early stages (Krivacic et al. 2004). However, traditional statistical bulk methods of cellular biology face sundry challenges when dealing with this case. Low quantity increases difficulties in precise and sensitive analysis of these heterogeneous cells within large number of unrelated cells (Vincent et al. 2010; Rane et al. 2012); for example, statistic methods that measure average responses from a population often obscure the difference from individual cells (Carlo and Lee 2006). Also, mechanical damages caused by bulk manipulations and

rough macro-scale operations direct on the delicate cells both will lead to loss of those rare precious specimens.

Among various microfluidic techniques that have been developed to meet these challenges, droplet microfluidics are the most commonly used due to its versatility and ease for quantitative analysis at single cell level (Theberge et al. 2010). Encapsulating cells into massive pico- to nano-liter scale droplets develops a brand new way to manipulate, transport, culture and real-time monitor, etc., different kinds of cells to fulfill various demands for cell-based researches and applications (Guo et al. 2010b; Zhao et al. 2009; Tsuda et al. 2009; Trivedi et al. 2009). These droplets are effective nano-laboratories that can accommodate single cells. Their high surface / volume ratio improves biomolecular transportation to enhance the performance of cell-based assays (Guo et al. 2012). These advantages make droplet microfluidics benefit subsequent pertinent researches toward those specific heterogeneous cells (Yin and Marshall 2012). Nevertheless, as droplets form when aqueous phase is monodispersed in oil phase on microfluidic chips, their liquid property induces several limits for downstream cellular biology research as cell carriers: (1) The cell encapsulated cannot be fixed at a steady position within the droplet; and (2) the suspended droplets are always spherical due to surface tension, so that microscopic images of cells inside are often distorted because of the bended light rays. These two drawbacks interfere with the precise observation for special heterogeneous cells. (3) Liquid droplets easily deform when applied external force, which still limits possible needed biochemical manipulations for cells encapsulated.

Herein, we reported a facile microfluidic approach to improve these situations. In consideration of its advantages in biocompatibility, low immune response and resemblance to natural extracellular matrix (ECM), hydrogel alginate is adopted for cell encapsulation (Rowley et al. 1999; Tan and Takeuchi 2007; Choi et al. 2007). After mild gelatinization of alginate with Ca^{2+} (Mørch et al. 2006), disk-like calcium alginate hydrogel beads are synthesized with different cells of preprocessed blood sample inside. These hydrogel beads not only retain advantages of droplets as compartmentalization at single cell level, but also enhance their unique merits to study latent cancer cells in the blood sample. First, as a kind of colloid, hydrogel beads immobilize the encapsulated cells inside. Together with their disk-like morphology comprised of plat top/bottom surface, cells can maintain a constant position under long-time continuous microscopy. Thus, precise and undistorted observation and image records can be obtained. Second, hydrogel beads' shell provides a structural support with high stiffness. This stability makes manipulations of cells steerable relative to the cell itself and further facilitates downstream sorting and enrichment for cancer cells from irrelative hematological cells. The robust shell outside the cell also blocks harmful external fluidic mechanical functions (Schmidt et al. 2008; Velasco et al. 2012).These two benefits can significantly reduce the loss of rare precious cell samples. On the other hand, porous structure of calcium alginate enhances permeability of the shell and thus enables small molecule transportation such as antibodies, fluorescence dyes or nutrition and waste of encapsulated cells (Um et al. 2008; Morimoto et al. 2009), which makes various cell-based processes possible to fulfill the needs of cellular assays. Compared to recently developed microfluidic chips for capture and enrichment of CTCs on which CTCs cannot be collected or manipulated easily for biological or biomedical analysis because of their irreversible adherence onto the specific substrates (Nagrath et al. 2007; Wang et al. 2011; Chen et al. 2011; Zhang et al. 2012b), compartmentalization of cells in hydrogel beads enables CTCs' isolation without using nano-structure-substrate-based bio-conjugate methods and thus can lead to more facile treatments and processes of CTCs. In this work, as a proof of conception for hydrogel bead-based stratagem, a commonly used three-color immunocytochemistry staining method, including FITC-labeled anti-CD45 (a marker for WBCs), PE-labeled anti-CK (cytokeratin, a protein marker for epithelial cells) and DAPI nuclear staining(Wang et al. 2009), was implemented based on these cell-encapsulated beads. This novel implementation could be used to identify cancer cells from white blood cells (WBCs). After integrated with other droplet-based methods of sorting (Guo et al. 2010a), cell culture (Liu et al. 2012), emulsion PCR (Leng et al. 2010), single cell gene detection and sequencing (Novak et al. 2011), etc., the beads containing target cells of heterogeneity could be separated and enriched individually, followed by pertinent analysis to gain more insights at cellular or molecular level. This hydrogel bead-based stratagem could facilitate enrichment, cultivation, sequencing and other downstream researches for CTCs or other rare specific cells from heterogeneous mixtures.

2 Experimental

2.1 Reagents and materials

Sodium alginate, sodium chloride and calcium chloride were purchased from China National Medicines Corporation Ltd. (China). Soybean oil (the immiscible continuous phase carrier) was purchased from Beiya Medical Oil Corporation Ltd. (China). Poly(dimethylsiloxane) (PDMS, RTV615) was purchased from GE Toshiba Silicone Corporation Ltd. (USA). All aqueous solutions were prepared using deionized water purified by a Millipore

Direct-Q3 water purification system (Millipore, MA, USA) and were filtered through 0.2-μm syringe filter to remove large clumps and bacteria. Dulbecco's modified Eagle's medium (DMEM, Hyclone, high glucose) and PBS (Hyclone, 1X, 0.0067 M PO_4^{3+}) were obtained from Thermo-Fisher Scientific; 0.25 % Trypsin–EDTA (Gibco, 1X), Tween-20 and fetal bovine serum were purchased from Invitrogen. Paraformaldehyde (PFA), Triton X-100, bovine serum albumin (BSA), normal goat serum and 4′,6-diamidino-2-phenylindole dihydrochloride (DAPI) were purchased from Sigma-Aldrich. Colorectal cell line (HCT116) and citrated whole blood samples from healthy donors were purchased from Zhongnan Hospital of Wuhan University. FITC-labeled anti-human CD45 (Ms IgG1, clone H130) (a marker for white blood cells) and PE-labeled anti-cytokeratin (CAM5.2, conjugated with phycoerythrin) (a marker for epithelial cells) were purchased from BD Bioscience.

2.2 Design and fabrication of microfluidic device

As shown in Fig. 1a, the microfluidic device is mainly made of two flow-focusing channels that produce sodium alginate and $CaCl_2$ droplets, respectively, and downstream merging chambers and channel to enable droplets merging and calcium alginate beads generation. Width of the middle inlet channels and the flow-focusing channels is at first 200 μm and then tapered to 50 μm near the orifice, while the two side channels tapered to 80 μm. Then, the channels expand from 50 to 80 μm. The downstream merging channel is 100 μm at the beginning, with two oval merging chambers whose width is 200 μm. Height of the microchannels is about 25 μm.

The mold was fabricated on a silicon wafer with SU-8 2050 photoresist (MicroChem Corporation, MA, USA) using a standard photolithographic method. Then, the PDMS layer was gained by using a conventional soft lithography technique (Xia and Whitesides 1998). After bonding the PDMS layer on a glass slide with oxygen plasma (Harrick Scientific Corporation, USA) treatment, the PDMS microfluidic device was baked at 120 °C for 12 h to regain hydrophobicity (Ji et al. 2011).

2.3 Cell culture, pretreatment of whole blood samples and preparation of sodium alginate cell suspension

The HCT116 cells were cultured in DMEM with 10 % FBS and 1 % penicillin and streptomycin at 37 °C and 5 % CO_2 atmosphere in a cell incubator (Thermo Forma Series II, Thermo Scientific). After harvested from the culture flask, HCT116 cells were centrifuged to remove the supernatant culture medium and then resuspended in 0.9 % (w/w) NaCl solution at needed concentrations.

The artificial CTC blood sample was made by mixing 0.5 mL HCT116 cell suspension in 0.9 % NaCl solution with 1 mL healthy donor's blood sample. And the cell density of HCT116 was adjusted to about 1×10^6/mL in the artificial blood sample.

Citrated blood sample (the artificial CTC blood sample) kept in anticoagulant tube (EDTA K_2, 2 mL, violet cap) (Wuhan Zhiyuan Medical Technology Corporation Ltd.) was mixed with equivalent Hank's solution completely and then added to the above of lymphocytes separation medium (Hao Yang Biological Manufacture Corporation Ltd., Tianjin, China) very slowly to maintain the liquid interface clearly. After centrifugation at 1,800 rpm for 30 min, the well-defined cloudy white nebulous strait lymphocyte layer at the interface, including lymphocytes and monocytes (also cancer cells in artificial blood samples), was collected into another centrifuge tube using a pipette. The cells were washed by 0.9 % (w/w) NaCl solution twice and then centrifuged and resuspended at needed concentration.

All cell suspension (cell line/artificial blood) was mixed with 3 % sodium alginate solution at the volume ratio of 1:2 to gain the sodium alginate cell suspension before loaded into the microfluidic device.

2.4 Generation of cell-encapsulated disk-like hydrogel beads

By using the previous-described device, disk-like hydrogel beads were generated containing different cells, that is, HCT116 cells, lymphocytes or other monocytes from blood samples. As shown in Fig. 1a, oil phase was introduced into the chip through inlets A1 and A2 by two syringe pumps (TS2-60, Longer Precision Pump Corporation Ltd.) through poly (tetrafluoroethylene) (PETE) tubes. Prepared sodium alginate cell suspension and 1 % (w/w) calcium chloride solution were injected from inlets B and C, respectively, and then sheared off into droplets at the flow-focusing orifice (Anna et al. 2003). Those droplets were directed into downstream merging channel and then merged in the expanded merging chambers because of velocity gradient. As the flow rates of continuous phase and dispersed phase could be precisely controlled, sodium alginate droplets were arrayed between the inter-spaces of $CaCl_2$ droplets (Fig. 2a). After the two kinds of droplets merged with each other, disk-like calcium alginate beads were generated due to cross-linking reaction between Ca^{2+} and alginate (Fig. 2b).

2.5 Hydrogel bead-based immunofluorescence staining

After generation within the microfluidic device, disk-like calcium alginate beads encapsulating cells were collected into a centrifuge tube at the outlet. Those beads were

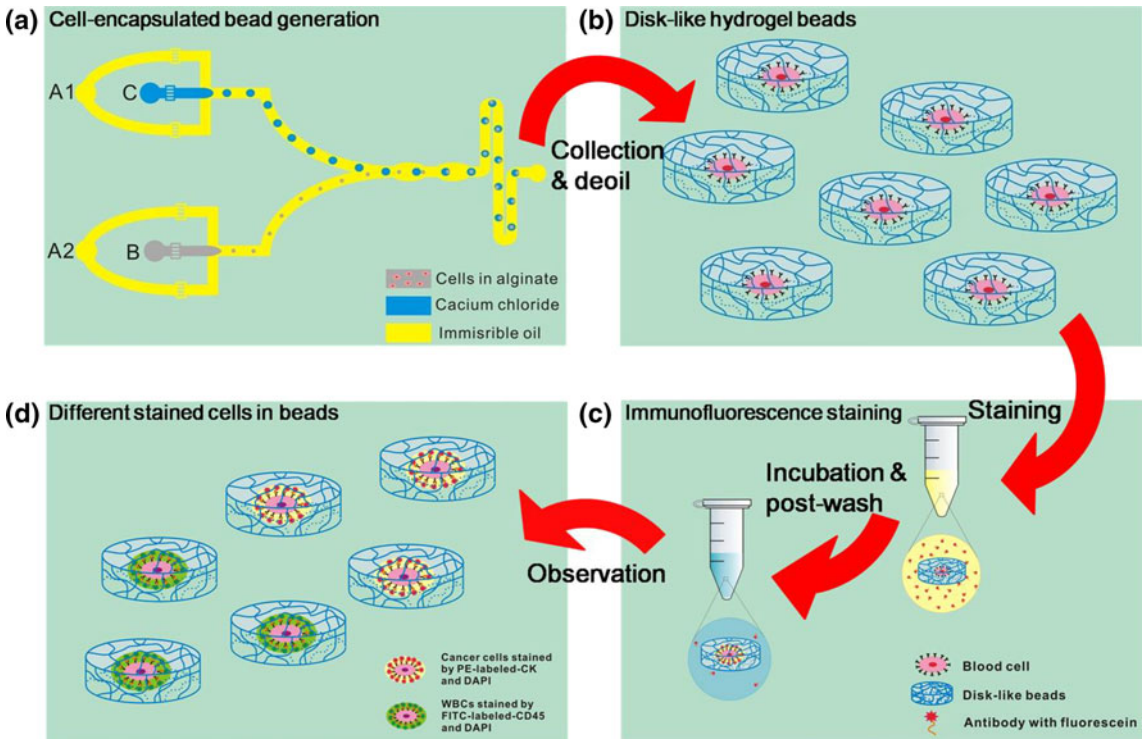

Fig. 1 Workflow diagram showing the disk-like hydrogel bead-based immunofluorescence staining. **a**, **b** Different kinds of blood cells were encapsulated in disk-like hydrogel beads. **c** After collected into centrifuge tube, immunofluorescence staining was implemented based on those cell-encapsulated hydrogel beads. **d** Different cells in blood showing distinct immunofluorescence within the disk-like beads

rinsed using 0.9 % NaCl solution and centrifuged at low speed to remove the oil for three times. Subsequently, 4 % PFA was added into the tube to fix cells for 20 min. Next, the beads were immersed in 0.2 % Triton X-100 for 10 min to increase cellular membrane permeability for intracellular staining. Then, blocking was carried out for 10 min using 5 % normal goat serum, 3 % bovine serum album and 0.1 % Tween-20 in 0.9 % NaCl solution as a blocker, which decreased nonspecific bonding during immunofluorescence staining. Finally, the beads were immersed in staining solution (10 μL anti-human CD45 and 10 μL anti-cytokeratin mixed with 80 μL blocker) at 4 °C in the dark for about 9 h and then stained with DAPI for another 10 min before observation. Between each step of fixation, permeabilization, blocking and staining, the calcium alginate beads were centrifuged to remove superfluous solution and washed by 0.9 % NaCl solution.

After staining, the beads containing cells were washed by 0.9 % NaCl solution for three times, then were resuspended in 0.9 % NaCl solution and added onto a glass slide for observation. The bright field and fluorescence images were monitored and recorded by a digital CCD camera mounted on an inverted fluorescence microscope (IX81, Olympus, Japan).

3 Results and discussion

3.1 Generation of disk-like hydrogel beads

Regulating the flow rates of fluids allows us to control the size of the hydrogel beads from tens to nearly one hundred of micrometers in diameter (Fig. 3), which can be adjusted according to the demand of different manipulations in various assays. Diameter of the hydrogel beads defines some important properties relating to the environment around the cells, such as permeability of the solute and intercellular communication (Sugiura et al. 2005; Kato et al. 2012).

In order to generate disk-like hydrogel beads, the diameter of every bead could be regulated to be larger than the height of the device's channel through controlling the flow rates of oil/alginate phase under predescribed dimensions of the flow-focusing orifice (Liu et al. 2006). As calcium alginate beads kept disk-like shape, their top surface and under surface were flat (Fig. 2c, d), which made the images of the cells encapsulated in the beads undistorted. Also, flat bottom of the disk-like beads could avoid rolling possibility of spherical beads. Due to the independent generation procedure of $CaCl_2$ droplets and sodium alginate ones, these two different kinds of droplets

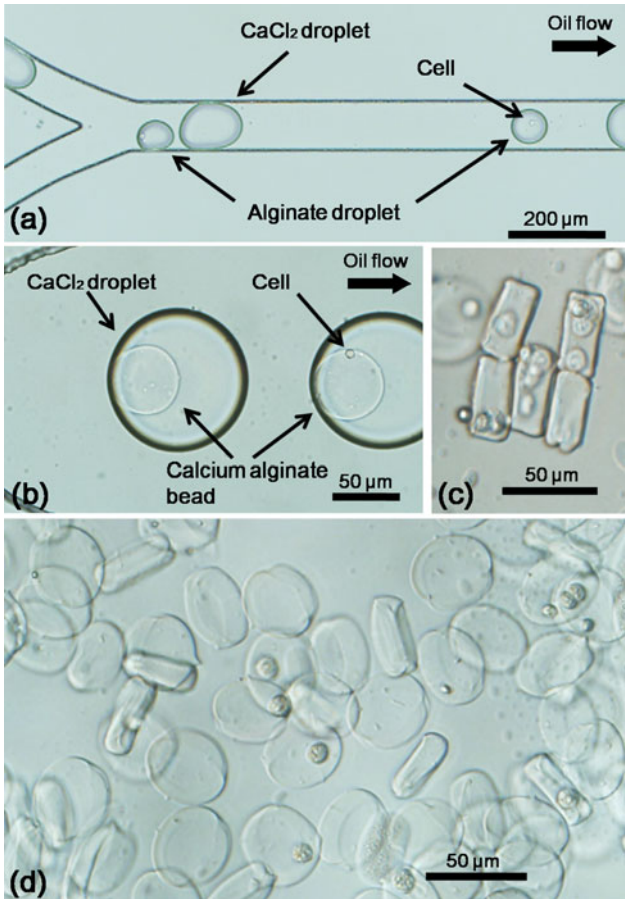

Fig. 2 Generation of disk-like hydrogel beads for cell encapsulation. **a** $CaCl_2$ droplets and sodium alginate ones were arrayed one after another alternately along the merging channel. **b** $CaCl_2$ droplet and sodium alginate droplets met and then merged with each other in the merging chambers, and disk-like calcium alginate beads were synthesized due to gelatinization reaction. **c**, **d** *Cross-section* and *top view* of disk-like hydrogel beads encapsulating cells

were arrayed one after another alternately along the merging channel before entering merging chambers and thus avoided the unwanted multiple merging among more than one sodium alginate droplets and insured the monodispersion of the beads' size (Fig. 2a). The expansion of merging chambers created velocity gradient interiorly, which made $CaCl_2$ droplet and sodium alginate droplets meet and then merge with each other. As Ca^{2+} ions served as cross-linking agents, gelatinization reaction happened when those two droplets merged, and the disk-like calcium alginate beads were then synthesized (Fig. 2b). At the same time, shrinkage of the beads would appear due to the cross-linking, so as the diameter of the beads decreased about 40 % than the sodium alginate droplets (Fig. 3). Meanwhile, after gelatinization, cells encapsulated are immobilized at a constant position within the beads, so more precise images can be obtained during continuous monitoring.

3.2 Cell encapsulation

In order to have good analysis or treatment for CTCs and eliminate possible influence of other cells, the cell number encapsulated in the disk-like beads was controlled to be single. Through adjusting cell density in sodium alginate and cell suspension mixture, the distribution of cells in droplets/beads was studied. The cell density influence on the cell encapsulation procedure was shown in Fig. 4a. Probability for the number of cells in every droplet was studied at five different cell densities. The experiment-determined distribution for number of cells per droplet at different cell densities (symbol) showed good fit with the Poisson distributions (dashed line) (Koster et al. 2008;

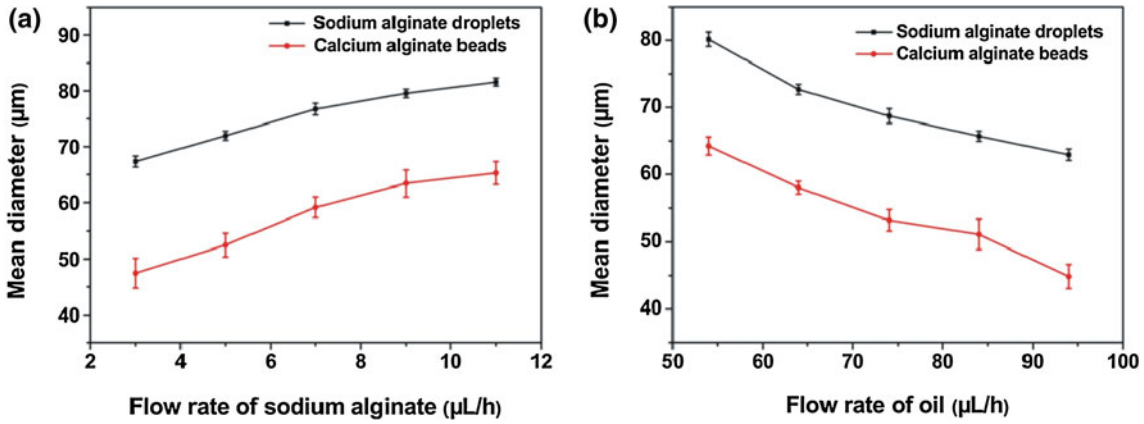

Fig. 3 The relationship between mean diameter of sodium alginate droplets (*black lines*)/calcium alginate beads (*red lines*) and flow rates of sodium alginate solution/oil. **a** Mean diameters changed with the flow rate variation of sodium alginate solution, when the flow rate of oil was fixed at 64 μL/h. **b** Mean diameters were controlled through adjusting the flow rate of oil, with the flow rate of sodium alginate solution fixed at 5 μL/h. A total of 50 sodium alginate droplets/calcium alginate beads were counted to provide every last average diameter and relative *error bar* (color figure online)

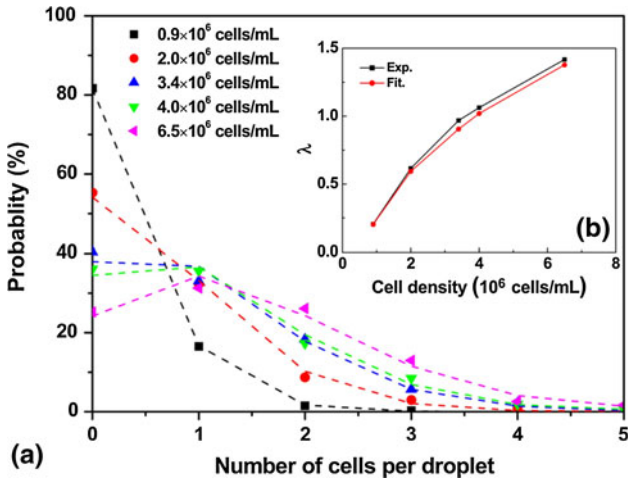

Fig. 4 The cell density influenced cell encapsulation procedure. **a** The probability for the number of cells in every droplet was studied at five different cell densities. The experiment-determined distribution for number of cells per droplet at different cell densities (*symbol*) showed good fit with the Poisson distributions (*dashed line*). **b** Average number of cells per droplet (λ) versus the five cell densities. The experiment data were showed by *black line* with theoretical values given by *red* one. A total of 500 droplets with/without cells were stochastically analyzed to gain the distribution of every last cell density (color figure online)

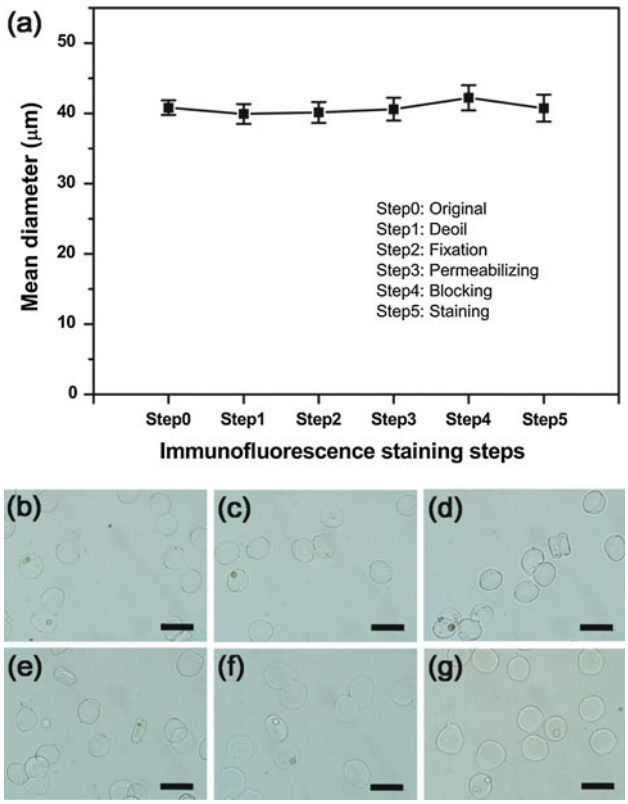

Fig. 5 Stability and morphology of hydrogel beads during whole procedure of deoil, fixation, permeabilization, blocking and incubation for staining. **a** The *curve* showed that the about −40 μm-size hydrogel beads held their diameter during immunofluorescence staining process. Microscopy indicates that morphology of the resultant beads (**b**) *changed little* after each staining manipulation step of deoil (**c**), fixation (**d**), permeabilization (**e**), blocking (**f**) and staining (**g**) (*scale bars* are 50 μm)

Clausell-Tormos et al. 2008), as well as the average number of cells per droplet (λ) versus the five cell densities (Fig. 4b). Though the possibility for droplets containing single cell increased with cell density and reached peak at about 4.0×10^6 cells/mL, droplets containing multiple cells also occupied a considerable part, which was unwanted for CTCs' single cell analysis. So, it was a better choice to keep the cell density at a lower level, such as 0.9×10^6 cells/mL and thus enabled the hydrogel beads containing single cell reach more than 90 % excluding the empty beads. Despite large portion of empty droplets, there was little impairment in this method for observation and manipulations, such as immunofluorescence staining and subsequent sorting, of those resultant beads encapsulating cells.

3.3 Stability of calcium alginate beads during staining treatment

To insure the calcium alginate beads to be a robust and stable carrier for the cells encapsulated inside, a series of observation and measurement was implemented during every step of immunofluorescence staining assay to evaluate the deformation of disk-like calcium alginate beads. It could be seen from Fig. 5 that during whole procedure of deoil, fixation, permeabilization, blocking and incubation for staining, and several wash and centrifugation steps, the 40-μm-diameter calcium alginate beads kept their shape and diameter quite well. It indicates that calcium alginate beads have good stability and tolerance for several chemical materials to be a good container for cells to conduct more biological assays.

3.4 Immunofluorescence staining assay

Figure 6 showed the bright field and fluorescence images of different cells in disk-like calcium alginate beads encapsulating HCT116 cell line and artificial blood sample, respectively. In these figures, HCT116 cells or CTCs (DAPI+/CK+/CD45−) could be easily distinguished from WBCs (DAPI+/CK−/CD45+) for their distinct fluorescence, which showed no difference with cells treated by traditional immunofluorescence staining method. This indicates that the calcium alginate shell outside the cells was permeable for small molecules (such as PFA, Triton X-100, Tween-20, DAPI) and proteins (BSA, antibodies, i.e., anti-CD45, anti-cytokeratin and so on) and would not impair their normal effects. It was obvious that there was

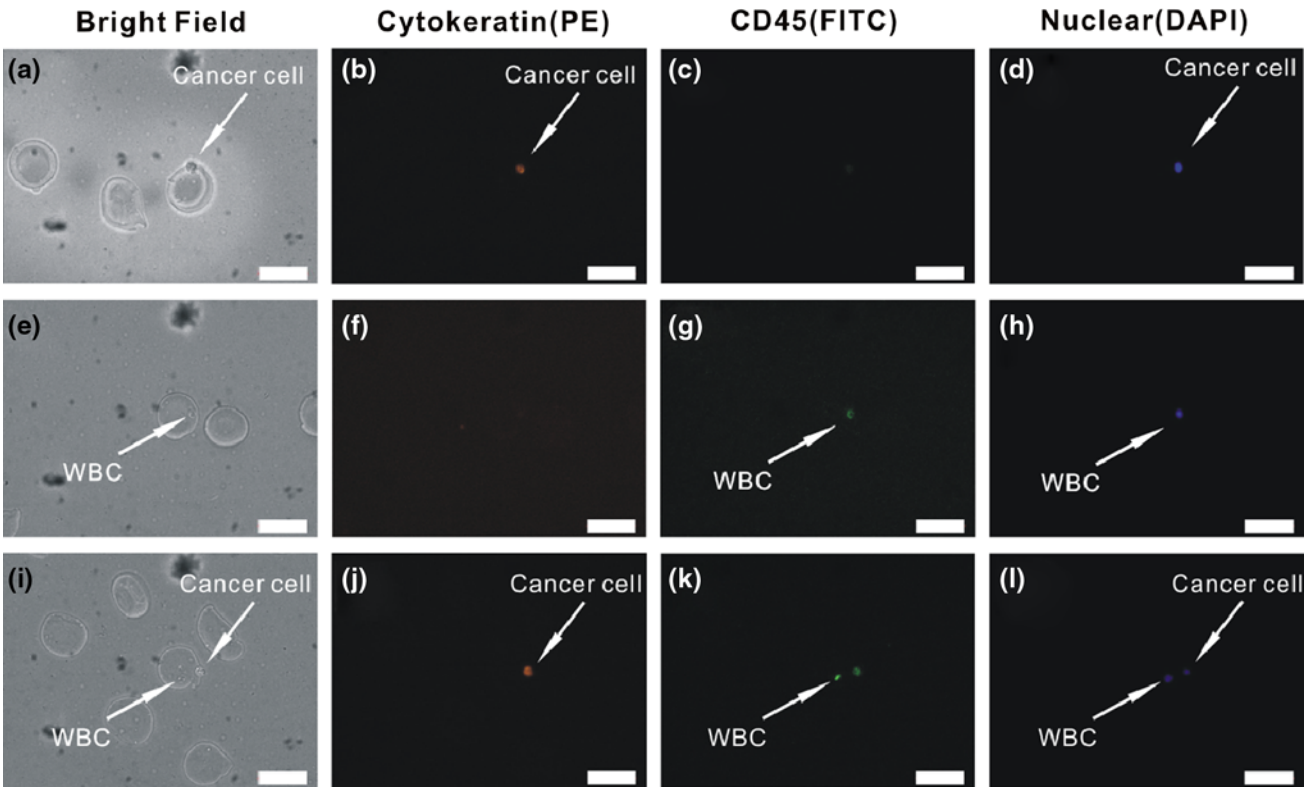

Fig. 6 Bright field and fluorescence images of different cells in disk-like calcium alginate beads encapsulating HCT116 cell line (**a**–**d**) and artificial blood sample (**e**–**l**), respectively, *after three-color* immunocytochemistry staining (*scale bars* are 50 μm). HCT116 cell line (**a**–**d**) or HCT116 cells in artificial blood sample (DAPI+/CK+/CD45−) (**e**–**h**) could be easily distinguished from white blood cells (WBCs) (DAPI+/CK−/CD45+) (**e**–**l**) from their distinct fluorescence, which showed no difference with cells treated by traditional immunofluorescence staining method. **i**–**l** Showed a hydrogel beads containing one HCT116 cancer cell and one WBC. It was obvious that there was little nonspecific absorption of the fluorescein-labeled anti-CD45, anti-cytokeratin and DAPI for calcium alginate beads

little nonspecific absorption of fluorescein-labeled anti-CD45, anti-cytokeratin and DAPI for calcium alginate beads. Also, calcium alginate showed very low fluorescence background noise to interfere the observation of cellular fluorescence. These properties made calcium alginate bead quite suitable for cell encapsulation and manipulations in many biological and biochemical assays.

4 Conclusion

In this paper, monodisperse disk-like hydrogel beads encapsulating different kinds of cells were synthesized, and immunofluorescence staining for the identification of cancer cells from normal cells in blood was implemented on the encapsulated cells through permeable calcium alginate shell, which demonstrated potential hydrogel bead-based biological and biochemical cell applications. Through modulating dimensions of fluidic channels and flow rates, disk-like calcium alginate beads of different sizes could be produced easily. Due to independent regulation of generation of $CaCl_2$ and sodium alginate droplets, synthesis of every calcium alginate bead was compartmentalized in the bigger $CaCl_2$ droplets, avoiding the adhesion of the beads effectively. With adjustment of cell density in sodium alginate solution, lot of single cell containing disk-like beads were gained, followed by the immunofluorescence staining assay for marking different cells. The assays indicate that calcium alginate beads not only provide mechanically and chemically stable shell for encapsulated cells against the harmful shear force or other hazardous external influences, but also avoid impairment of the normal biological or biochemical manipulations for cells inside at the same time, for example, obstruction or absorption of fluorescein-labeled antibodies or high fluorescence background noise. As a uniqueness, the plat top/bottom surface of beads' disk-like shape provided clear observation and record for bright field and fluorescence images. After integration with lots of other manipulation methods for droplets/beads, this platform could have potential applications for sorting, culture, single cell analysis, etc., of CTCs or other specific cells from heterogeneous mixtures on single cell level.

Acknowledgments This work was supported by National Natural Science Foundation of China (Grant No. 81272443), the State Key

Program of National Natural Science of China (Grant No. 51132001) and National Science Fund for Talent Training in Basic Science (Grant No. J1210061). The authors would like to acknowledge Dr. Nangang Zhang (School of Physics and Technology, Wuhan University), Yuan Fang (the 2nd School of Clinical Medicine, Wuhan University) and Dr. Xinghu Ji (School of Chemistry and Molecular Sciences, Wuhan University) for lots of beneficial discussion.

References

Anna SL, Bontoux N, Stone HA (2003) Formation of dispersions using "flow focusing" in microchannels. Appl Phys Lett 82(3): 364–366

Asano M, Toda M, Sakaguchi N, Sakaguchi S (1996) Autoimmune disease as a consequence of developmental abnormality of a T cell subpopulation. J Exp Med 184(2):387–396

Carlo DD, Lee LP (2006) Dynamic single-cell analysis for quantitative biology. Anal Chem 78(23):7918–7925

Chen L, Liu X, Su B, Li J, Jiang L, Han D, Wang S (2011) Aptamer-mediated efficient capture and release of T lymphocytes on nanostructured surfaces. Adv Mater 23(38):4376–4380

Choi C-H, Jung J-H, Rhee Y, Kim D-P, Shim S-E, Lee C-S (2007) Generation of monodisperse alginate microbeads and in situ encapsulation of cell in microfluidic device. Biomed Microdevices 9(6):855–862

Clausell-Tormos J, Lieber D, Baret J-C, El-Harrak A, Miller OJ, Frenz L, Blouwolff J, Humphry KJ, Köster S, Duan H, Holtze C, Weitz DA, Griffiths AD, Merten CA (2008) Droplet-based microfluidic platforms for the encapsulation and screening of mammalian cells and multicellular organisms. Chem Biol 15(5): 427–437

Guo F, Ji X-H, Liu K, He R-X, Zhao L-B, Guo Z-X, Liu W, Guo S-S, Zhao X-Z (2010a) Droplet electric separator microfluidic device for cell sorting. Appl Phys Lett 96(19):193701–193703

Guo F, Liu K, Ji X-H, Ding H-J, Zhang M, Zeng Q, Liu W, Guo S-S, Zhao X-Z (2010b) Valve-based microfluidic device for droplet on-demand operation and static assay. Appl Phys Lett 97(23):233701–233703

Guo MT, Rotem A, Heyman JA, Weitz DA (2012) Droplet microfluidics for high-throughput biological assays. Lab Chip 12(12):2146–2155

Gupta GP, Massagué J (2006) Cancer metastasis: building a framework. Cell 127(4):679–695

Ji X-H, Cheng W, Guo F, Liu W, Guo S-S, He Z-K, Zhao X-Z (2011) On-demand preparation of quantum dot-encoded microparticles using a droplet microfluidic system. Lab Chip 11(15):2561–2568

Kato A, Yanagisawa M, Sato YT, Fujiwara K, Yoshikawa K (2012) Cell-sized confinement in microspheres accelerates the reaction of gene expression. Sci Rep 2:283. doi:10.1038/srep00283

Koster S, Angile FE, Duan H, Agresti JJ, Wintner A, Schmitz C, Rowat AC, Merten CA, Pisignano D, Griffiths AD, Weitz DA (2008) Drop-based microfluidic devices for encapsulation of single cells. Lab Chip 8(7):1110–1115

Krivacic RT, Ladanyi A, Curry DN, Hsieh HB, Kuhn P, Bergsrud DE, Kepros JF, Barbera T, Ho MY, Chen LB, Lerner RA, Bruce RH (2004) A rare-cell detector for cancer. Proc Natl Acad Sci USA 101(29):10501–10504

Leng X, Zhang W, Wang C, Cui L, Yang CJ (2010) Agarose droplet microfluidics for highly parallel and efficient single molecule emulsion PCR. Lab Chip 10(21):2841–2843

Liu K, Ding H-J, Liu J, Chen Y, Zhao X-Z (2006) Shape-controlled production of biodegradable calcium alginate gel microparticles using a novel microfluidic device. Langmuir 22(22):9453–9457

Liu K, Deng Y, Zhang N, Li S, Ding H, Guo F, Liu W, Guo S, Zhao X-Z (2012) Generation of disk-like hydrogel beads for cell encapsulation and manipulation using a droplet-based microfluidic device. Microfluid Nanofluid 13(5):761–767

Mørch ÝA, Donati I, Strand BL (2006) Effect of Ca^{2+}, Ba^{2+}, and Sr^{2+} on alginate microbeads. Biomacromolecules 7(5):1471–1480

Morimoto Y, W-h Tan, Tsuda Y, Takeuchi S (2009) Monodisperse semi-permeable microcapsules for continuous observation of cells. Lab Chip 9(15):2217–2223

Nagrath S, Sequist LV, Maheswaran S, Bell DW, Irimia D, Ulkus L, Smith MR, Kwak EL, Digumarthy S, Muzikansky A, Ryan P, Balis UJ, Tompkins RG, Haber DA, Toner M (2007) Isolation of rare circulating tumour cells in cancer patients by microchip technology. Nature 450(7173):1235–1239

Novak R, Zeng Y, Shuga J, Venugopalan G, Fletcher DA, Smith MT, Mathies RA (2011) Single-cell multiplex gene detection and sequencing with microfluidically generated agarose emulsions. Angew Chem Int Ed 50(2):390–395

Rane TD, Zec HC, Puleo C, Lee AP, Wang T-H (2012) Droplet microfluidics for amplification-free genetic detection of single cells. Lab Chip 12(18):3341–3347

Rowley JA, Madlambayan G, Mooney DJ (1999) Alginate hydrogels as synthetic extracellular matrix materials. Biomaterials 20(1): 45–53

Schmidt JJ, Rowley J, Kong HJ (2008) Hydrogels used for cell-based drug delivery. J Biomed Mater Res Part A 87A(4):1113–1122

Sugars KL, Rubinsztein DC (2003) Transcriptional abnormalities in Huntington disease. Trends Genet 19(5):233–238

Sugiura S, Oda T, Izumida Y, Aoyagi Y, Satake M, Ochiai A, Ohkohchi N, Nakajima M (2005) Size control of calcium alginate beads containing living cells using micro-nozzle array. Biomaterials 26(16):3327–3331

Tan WH, Takeuchi S (2007) Monodisperse alginate hydrogel microbeads for cell encapsulation. Adv Mater 19(18):2696–2701

Theberge AB, Courtois F, Schaerli Y, Fischlechner M, Abell C, Hollfelder F, Huck WTS (2010) Microdroplets in microfluidics: an evolving platform for discoveries in chemistry and biology. Angew Chem Int Ed 49(34):5846–5868

Trivedi V, Ereifej ES, Doshi A, Sehgal P, VandeVord PJ, Basu AS (2009) Microfluidic encapsulation of cells in alginate capsules for high throughput screening. In: Engineering in Medicine and Biology Society, 2009. EMBC 2009. Annual International Conference of the IEEE, 3–6 September 2009, pp 7037–7040

Tsuda Y, Morimoto Y, Takeuchi S (2009) Monodisperse cell-encapsulating peptide microgel beads for 3D cell culture. Langmuir 26(4):2645–2649

Um E, Lee D-S, Pyo H-B, Park J-K (2008) Continuous generation of hydrogel beads and encapsulation of biological materials using a microfluidic droplet-merging channel. Microfluid Nanofluid 5(4):541–549

Velasco D, Tumarkin E, Kumacheva E (2012) Microfluidic encapsulation of cells in polymer microgels. Small 8(11):1633–1642

Vincent ME, Liu W, Haney EB, Ismagilov RF (2010) Microfluidic stochastic confinement enhances analysis of rare cells by isolating cells and creating high density environments for control of diffusible signals. Chem Soc Rev 39(3):974–984

Wang S, Wang H, Jiao J, Chen K-J, Owens GE, Kamei K-i, Sun J, Sherman DJ, Behrenbruch CP, Wu H, Tseng H-R (2009) Three-dimensional nanostructured substrates toward efficient capture of circulating tumor cells. Angew Chem 121(47):9132–9135

Wang S, Liu K, Liu J, Yu ZTF, Xu X, Zhao L, Lee T, Lee EK, Reiss J, Lee Y-K, Chung LWK, Huang J, Rettig M, Seligson D, Duraiswamy KN, Shen CKF, Tseng H-R (2011) Highly efficient capture of circulating tumor cells by using nanostructured silicon substrates with integrated chaotic micromixers. Angew Chem Int Ed 50(13):3084–3088

Xia Y, Whitesides GM (1998) Soft lithography. Angew Chem Int Ed 37(5):550–575

Yin H, Marshall D (2012) Microfluidics for single cell analysis. Curr Opin Biotechnol 23(1):110–119

Zhang H, Jenkins G, Zou Y, Zhu Z, Yang CJ (2012a) Massively parallel single-molecule and single-cell emulsion reverse transcription polymerase chain reaction using agarose droplet microfluidics. Anal Chem 84(8):3599–3606

Zhang N, Deng Y, Tai Q, Cheng B, Zhao L, Shen Q, He R, Hong L, Liu W, Guo S, Liu K, Tseng H-R, Xiong B, Zhao X-Z (2012b) Electrospun TiO_2 nanofiber-based cell capture assay for detecting circulating tumor cells from colorectal and gastric cancer patients. Adv Mater 24(20):2756–2760

Zhao LB, Pan L, Zhang K, Guo SS, Liu W, Wang Y, Chen Y, Zhao XZ, Chan HLW (2009) Generation of janus alginate hydrogel particles with magnetic anisotropy for cell encapsulation. Lab Chip 9(20):2981–2986

Zhu J, Nguyen T, Pei R, Stojanovic M, Lin Q (2012) Specific capture and temperature-mediated release of cells in an aptamer-based microfluidic device. Lab Chip 12(18):3504–3513